

# Control of Adsorption State Based on Conformational Change of Poly(methacrylic acid)-Functionalized, Double-Chain Monolayers on Gold Substrates

Masazo Niwa,\* Toshiaki Mori, and Nobuyuki Higashi

Department of Applied Chemistry, Faculty of Engineering, Doshisha University, Kamikyo-ku, Kyoto 602, Japan

Received October 21, 1992; Revised Manuscript Received December 28, 1992

**ABSTRACT:** Polymeric amphiphiles ( $1_n$ ) containing poly(methacrylic acid) (PMAA) segments having different chain lengths ( $n = 35, 63$ , and  $177$ ) and two long alkyl chains whose ends are modified with disulfide groups are newly prepared, and ellipsometric and electrochemical studies of the  $1_n$  monolayer-covered gold substrates are described. The  $1_n$  are spontaneously adsorbed onto gold substrates from aqueous solutions with various pHs and form monolayer assemblies. The ellipsometric thickness of the resulting monolayers is markedly affected by the PMAA chain length ( $n$ ) and/or the surrounding pH during adsorption: the thicknesses increase both with increasing  $n$  and with increasing pH. These changes in thickness are governed by the conformation of the PMAA segments since the data can be rationalized in terms of the molecular size of the PMAA segments based on their extent in the conformational state. Electrochemical redox measurements on the monolayers provide information about the lateral orientation (molecular packing) of  $1_n$  within the monolayers. The data suggest that the packing density of  $1_{63}$  in the monolayer adsorbed at pH 3.0 is much higher than that adsorbed at pH 8.2, reflecting the conformational size of the PMAA segment adopted at each pH. The immobilized monolayer on the gold substrate gives reversible changes in the ellipsometric thickness and in the electrochemical response by varying pH, though the changes are dependent upon the molecular packing density on the substrates.

## Introduction

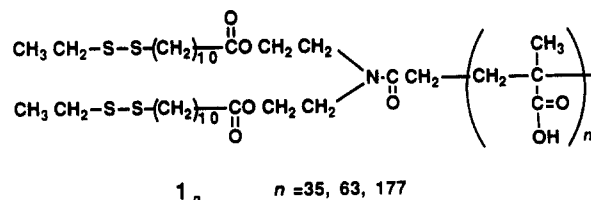
For many years, much effort has been dedicated to the study of macromolecules carrying ionized or ionizable groups. These synthetic polyelectrolytes are important in many industrial applications and also as simplified models of natural polyelectrolytes. Poly(methacrylic acid) (PMAA) shows a marked pH-induced conformational change:<sup>1</sup> at low pH the macromolecule adopts a hypercoiled form to minimize the hydrophobic interactions, and at a higher degree of ionization (higher pH) and in the absence of electrolytes, the PMAA chain stretches to an expanded form. Recently, polyelectrolytes grafted to a solid substrate (*polyelectrolyte brushes*) have been theoretically demonstrated in terms of their physical and physico-chemical properties.<sup>2-5</sup>

We have focused on the design and preparation of polymeric amphiphiles carrying a polyelectrolyte segment such as PMAA and their monolayer properties at the air-water interface.<sup>6-11</sup> These polymer assemblies have provided characteristics uniquely different from those in homogeneous media. Amphiphiles of PMAA connected at one terminus with hydrophobic polymers or long alkyl chains have been aligned at the air-water interface, and their monolayer state could be controlled by the conformational change of the PMAA segment.<sup>10</sup> Furthermore, PMAA monolayers were found to recognize the chain length of corresponding guest polymers such as poly(ethylene glycol) added to the subphase mainly due to multiple hydrogen bonding between polymers.<sup>10</sup> Similar situations were observed for other combinations of host polymer monolayers and guest polymers.<sup>11-13</sup> Recently, we have found that a poly(L-glutamic acid)-functionalized, double-chain amphiphile forms unprecedented conformations at the air-water interface by assembling the polymer segment.<sup>14</sup>

As part of our research into the conformational properties of polyelectrolyte chains embedded in molecular assemblies, we have newly prepared polymeric amphiphiles ( $1_n$ ) containing a PMAA segment and two long alkyl chains whose ends are modified with disulfide groups to attach

to a gold surface and reveal conformational behaviors in the adsorbed monolayer state on gold substrates. It has been shown that well-organized monolayers can be readily prepared on gold by spontaneous adsorption of organic thiols and disulfides.<sup>15-22</sup> This method has been used to modify the surface properties of gold and also to prepare functional gold electrodes. Actually, we have shown that SH-terminated PMAA can be adsorbed onto a gold electrode and that the conformational change of PMAA is monitored electrochemically, though the blocking ability of this polymer monolayer to redox couples is not so high.<sup>23</sup> Octadecanethiol monolayers are strongly blocking to many redox couples in aqueous electrolytes.<sup>24-29</sup> Sabatini et al.<sup>26,27</sup> have demonstrated that the thiol monolayer-coated electrode behaves like a microelectrode array. Pinholes in the organized monolayer function effectively as microelectrodes.

We describe here the preparation and adsorption state of novel PMAA-functionalized monolayers ( $1_n$ ) which contain two long alkyl chains to improve molecular ordering on a gold surface and to separate the gold-adsorbable moiety ( $-S-S-$ ) and the conformational-changeable moiety (PMAA segment). In this system, it is expected that adsorption processes of  $1_n$  onto gold will be controlled on the basis of conformational change and/or segment length of PMAA and the resulting monolayers will be applicable to microelectrodes.



## Experimental Section

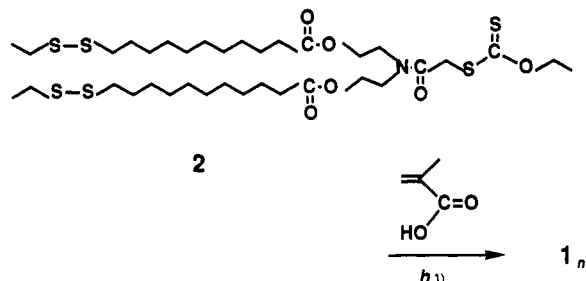
**Materials. Preparation of  $1_n$ .** The polymeric amphiphiles ( $1_n$ ) were prepared according to the following scheme. Xanthate

**Table I**  
Polymerization Conditions and Characterization of  
Amphiphilic Polymers ( $1_n$ )

run	feed comp <sup>a</sup> [MMA]/[2] <sub>0</sub>	irrad time <sup>b</sup> (h)	conv (%)	$x^c$ (mmol g <sup>-1</sup> )	$n^d$
1	30.3	24	18	9.20	35
2	58.8	24	28	10.2	63
3	111.1	24	27	11.1	177

<sup>a</sup> [MAA]<sub>0</sub> = 1.0 M. <sup>b</sup> Photopolymerizations were carried out in methanol at 30 °C; irradiation source, low-pressure Hg lamp. <sup>c</sup>  $x$  is the content of the MAA unit in the polymer molecule. <sup>d</sup> Number-average degree of polymerization ( $n$ ) calculated by the following equation:  $n = M_2x/(10^3 - M_m x)$ ;  $M_2$  and  $M_m$ , molecular weight of 2 and MAA, respectively.

derivatives such as 2 can serve as an effective photoinitiator-transfer agent-terminator for the polymerization of vinyl monomers, and thus the chain length of the resulting polymer can be sufficiently controlled by adjusting the feed composition of initiator and monomer and the conversion of monomer.<sup>30</sup>



The preparation of photoinitiator 2 (*O*-ethyl *S*-[[*N,N*-bis[2-[(11-ethyldithioundecanoyl)oxy]ethyl]carbamoyl]methyl] dithiocarbonate) has been described elsewhere.<sup>22</sup>

The photopolymerizations of methacrylic acid (MAA) were carried out in a glass ampule under a nitrogen atmosphere upon UV irradiation (light source: low-pressure Hg lamp) with 2 and methanol as solvent. The obtained polymers were purified by reprecipitation from methanol (solvent) and benzene (nonsolvent). The number-average degree of polymerization ( $n$ ) of the PMAA segment was determined by estimating the content of MAA units in the polymer molecule by a conductometric titration with aqueous NaOH. The polymerization conditions and characterization of polymers obtained are summarized in Table I.

**Preparation of Ferrocenecarboxylic Acid 1-Glycerol Ester (Fc-Gly).** *dl*-Isopropylideneglycerol was prepared according to the literature.<sup>31</sup> Ferrocenecarbonyl chloride was prepared as follows. A benzene solution (20 mL) of 4.4 g of oxalyl chloride (35 mmol) was added dropwise with ice cooling to a benzene solution (80 mL) containing ferrocenecarboxylic acid (2.0 g, 9 mmol) and a small amount of pyridine. The mixture was additionally stirred for 26 h at room temperature. After removal of solvent and excess oxalyl chloride, the residue was extracted with hexane. The solvent was removed, and a red-yellow crystal was obtained: yield 1.8 g (81%); IR 1760 cm<sup>-1</sup> ( $\nu_{C=O}$ , acid chloride).

*dl*-Isopropylideneglycerol (0.75 g, 5.7 mmol) and 0.5 g of pyridine (6 mmol) were dissolved in benzene (20 mL), and 1.7 g (6.8 mmol) of ferrocenecarbonyl chloride in benzene (20 mL) was added dropwise. The mixture was additionally stirred for 110 h at room temperature, and then the salt produced was removed. After solvent removal, the residue was extracted with hexane. The solvent was removed, and a yellow crystal was obtained: yield 2.0 g (73%); IR 1720 cm<sup>-1</sup> ( $\nu_{C=O}$ , ester).

The ester (1.4 g, 4.1 mmol) thus obtained was dispersed in 10% acetic acid (500 mL) and then stirred for 8 h at 60 °C. The reaction mixture was added into ether, and the ether layer was separated and dried. After solvent removal, the residue was recrystallized from an ether-benzene mixture, giving a yellow crystal: yield 1.3 g (86%); IR 3400 ( $\nu_{OH}$ ), 1720 ( $\nu_{C=O}$ , ester), 1010 cm<sup>-1</sup> ( $\nu_{C-C}$ , ferrocene), disappearance of a peak at 1050 cm<sup>-1</sup> ( $\nu_{C-O-C}$ , ketal).

**Preparation of Monolayers on Gold Substrates.** Monolayers were spontaneously formed by immersing gold-mirror

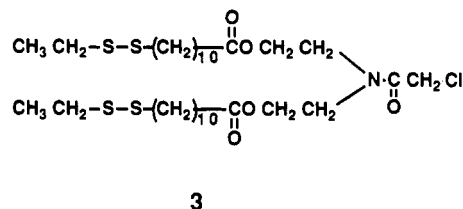
plates, which were prepared by evaporation of gold onto glass plates or clean gold electrodes, into a 1 mM solution of  $1_n$  in water (purified with a Milli-Q purification system, Millipore) with a prescribed pH. After a prescribed period, the gold substrates were removed and rinsed with clean water.

**Ellipsometric Film-Thickness Measurements.** Thicknesses of the films were determined with ellipsometry. Ellipsometry was performed at a 70° angle of incidence on a manual nulling ellipsometer with a He-Ne laser source. Samples were washed with water with a prescribed pH and blown dry with nitrogen before the measurements were taken. The ellipsometric parameters  $\psi$  and  $\Delta$  were measured on each gold mirror immediately before and after monolayer deposition. Eight separate points were measured on each sample and the readings then averaged. Film thicknesses were calculated from changes in  $\Delta$  and  $\psi$  by assuming an isotropic film with a refractive index of 1.49 for PMAA or 1.45 for alkyl chains. When the film thicknesses were computed by using each value, the calculated difference in the thickness was within 1 Å for all samples used in this study.

**Electrochemical Measurements.** Cyclic voltammetry was performed with a CV-1B cyclic voltammograph (BAS) and an RW-21 X-Y recorder (Rikadenki, Tokyo). The gold electrodes were mounted in a conventional three-electrode cell with an exposed area of 0.02 cm<sup>2</sup>. Solutions were purged with nitrogen. All potentials were measured and reported with respect to a Ag/AgCl (saturated KCl) reference electrode. Solutions were prepared immediately before use with deionized water from a Milli-Q purification system. pHs of the solutions were adjusted with the required amounts of HCl and NaOH. KCl and [Ru(NH<sub>3</sub>)<sub>6</sub>]Cl<sub>3</sub> were reagent grade.

## Results and Discussion

**Monolayer Formation and Characterization with Ellipsometry.** Three types of polymeric amphiphiles  $1_n$  with different PMAA chain lengths ( $n = 35, 63$ , and 177) were successfully prepared and used for the adsorption experiments. The assembling process and the resulting monolayer of  $1_n$  on gold should be affected by the chain length ( $n$ ) of the PMAA segment as well as the pH of the aqueous solution, since PMAA in aqueous media caused a marked conformational change by varying pH. Ellipsometry was applied as a convenient and precise means of determining the average monolayer thickness of the films. After complete adsorption (24 h) of  $1_n$  onto the gold mirror plate at pHs 3.0 and 8.2, the gold substrates were rinsed with pure water of the prescribed pH and dried for the ellipsometric measurement. Adsorption processes of  $1_n$  will be described in detail later. Figure 1 shows the ellipsometric thicknesses for  $1_n$  adsorbed on gold at pHs 3.0 and 8.2 as a function of the PMAA chain length ( $n$ ) of  $1_n$ . For comparison, the data of 3 monolayer (without PMAA segment) adsorbed at gold from ethanol solution was included as  $n = 0$  in the figure. The observed



thickness of 3 monolayer ( $23 \pm 3$  Å) was in good agreement with a molecular length of 23 Å estimated from a CPK molecular model. Therefore, the monolayer is considered to be an ideal film consisting of 3 molecule packed densely and oriented perpendicularly to the gold surface. Single long-chain thiols or disulfides have been found to form a monolayer assembly with fully extended alkyl chains tilted from the gold surface normal by 20–30°. <sup>29</sup> The structural

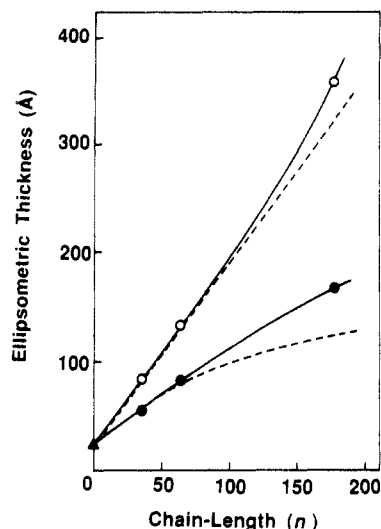


**Figure 1.** Film thicknesses for  $1_n$  adsorbed onto gold at pHs 3.0 (●) and 8.2 (○); the ellipsometrically determined thickness (—) and the estimated thickness obtained by taking account into the chain extent of the PMAA segment at the prescribed chain length ( $n$ ) and pH using the data of Oth et al.<sup>32</sup> (---) are plotted against the chain length ( $n$ ) of the PMAA segment. Solid triangle (▲) indicates the data of 3.

difference between them and our disulfide exists in the number of alkyl chains and thus the formation of an ideal film may result from the double-chained structure of 3.

As can be seen from the figure, the ellipsometric thickness increases with increasing PMAA chain length of  $1_n$ . Furthermore, the monolayers adsorbed at pH 8.2 are always thicker than those adsorbed at pH 3.0. These trends of the monolayer thicknesses must be due to a contribution from the molecular size of the PMAA segments on the basis of their extent in the conformational state (conformational size of the PMAA segment).

To elucidate the conformational effect of the PMAA segment of  $1_n$  on the resulting monolayer thickness, a mean molecular size of PMAA in aqueous solution was simulated by using the data of Oth et al.<sup>32</sup> The molecular size was estimated as the diameter of PMMA in a spherical form, taking account into the chain length ( $n$ ) and the surrounding pH. These simulated thicknesses, as the sum of 23 Å (thickness of 3 monolayer) and the estimated diameter of the PMAA segment, are shown in Figure 1 as dashed lines. The ellipsometrically determined thicknesses are consistent with the simulated thicknesses, though a slight deviation between them is observed for the monolayers with a longer PMAA chain ( $1_{177}$ ). These ellipsometric data clearly indicate that the monolayer thickness is governed by the conformational size of the PMAA segment, which can be readily changed by varying the segment length ( $n$ ) and the surrounding pH during adsorption.

It is also expected that a lateral orientation of  $1_n$  molecules in the monolayers as well as the monolayer thickness will be controllable by the conformational size of the PMAA segment.

**Conformational Effects of PMAA Segment on Lateral Orientation in Monolayers.** To evaluate the contribution of the conformational size of the PMAA segment to the monolayer structure such as lateral orientation and packing of  $1_n$ , electrochemical measurements were made. First, the adsorption process of  $1_n$  onto gold electrodes was revealed electrochemically. For the initial electrochemical run, Fc-Gly was selected and freshly prepared, since it is water-soluble and nonionic and ferrocene derivatives represent a convenient and electro-

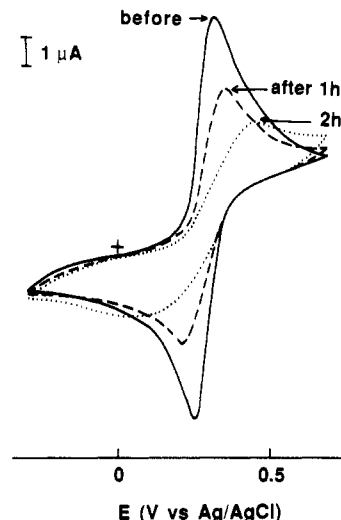


**Figure 2.** Cyclic voltammograms before (bare gold) and after immersion of the gold electrode into a solution of  $1_{63}$  at pH 3.0. The electrolyte solutions are 3 mM Fc-Gly in 1 M KCl, pH 3.0. The sweep rate is 70 mV/s.

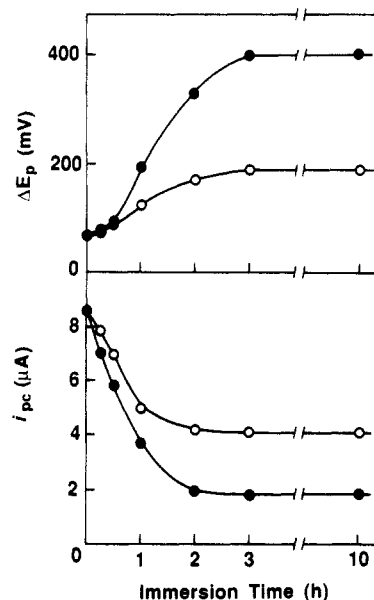


**Figure 3.** Changes in the values of  $i_{pc}$  and  $\Delta E_p$  upon immersion of the gold electrodes into solutions of  $1_{63}$  at pHs 3.0 (●) and 8.2 (○). Experimental conditions are the same as described in Figure 2.

chemically reversible, one-electron redox couple. The solid line in Figure 2 shows the cyclic voltammetric current-potential ( $i$ - $E$ ) responses for bare gold with 3 mM Fc-Gly as the electroactive species and with 1 M KCl as the electrolyte. The shape of the  $i$ - $E$  curve and 60-mV separation between the cathodic and anodic peak currents are indicative of a diffusion-limited or electrochemically reversible one-electron redox process.<sup>33</sup> Upon immersion of the electrode into an aqueous solution (pH 3.0) of  $1_{63}$ , a typical sample, the voltammograms showed an apparent decrease of the redox peak currents and an increase of the peak-to-peak separation, which indicated that contact of Fc-Gly with the electrode surface was restricted. To determine conditions under which steady-state monolayers are formed, the maximum reduction currents ( $i_{pc}$ ) and the peak-to-peak separation ( $\Delta E_p$ ) were plotted against immersion time for the case of  $1_{63}$  solutions (Figure 3). Steady-state adsorption is found to be reached after 3-h immersion at both pHs 3.0 and 8.2. There is, however, a significant difference in the values of  $i_{pc}$  and  $\Delta E_p$  at a

**Table II**  
Comparison of the Values of  $i_{pc}$  and  $\Delta E_p$  at a Steady-State Adsorption of  $1_n$

chain length of $1_n$ ( $n$ )	prepared at pH 3.0			prepared at pH 8.2		
	time <sup>a</sup> (h)	$i_{pc}$ <sup>b</sup> ( $\mu$ A)	$\Delta E_p$ <sup>c</sup> (mV)	time <sup>a</sup> (h)	$i_{pc}$ <sup>b</sup> ( $\mu$ A)	$\Delta E_p$ <sup>c</sup> (mV)
35	2	1.5	480	2	2.3	320
63	3	1.9	400	3	4.1	190
177	3	2.5	290	3	7.6	110

<sup>a</sup> Immersion time required for a steady-state adsorption. <sup>b</sup> Maximum reduction current. <sup>c</sup> Separation between the cathodic and anodic peak currents.

steady-state adsorption between pHs 3.0 and 8.2; i.e., the  $1_{63}$  electrode prepared at pH 3.0 gives a higher electrochemical barrier capability toward Fc-Gly relative to the electrode prepared at pH 8.2. This result suggests that the conformational size of the PMAA segment adopted at each pH affects the packing density of the monolayer. The same experiments were carried out for the other amphiphiles having a shorter PMAA length ( $1_{35}$ ) and a longer PMAA length ( $1_{177}$ ) relative to  $1_{63}$ . The values of  $i_{pc}$  and  $\Delta E_p$  at a steady-state adsorption are given in Table II. The steady-state monolayers were obtained within 3 h of immersion for all  $1_n$ 's. With increasing chain length of the PMAA segment ( $n$ ), the  $i_{pc}$  increased whereas the  $\Delta E_p$  decreased at both pHs 3.0 and 8.2. More drastic changes in such electrochemical parameters were observed between pHs 3.0 and 8.2. The barrier capability toward Fc-Gly was always higher for the monolayer prepared at pH 3.0 than that for the monolayer prepared at pH 8.2. This trend was more marked for the monolayer with the longer PMAA segment length. As mentioned earlier, PMAA adopts a hydrophobic, tightly coiled conformation at a low pH and is in an expanded state at a high pH. The results obtained thus clearly indicate that a lateral distribution of electroactive (or blocking) sites based on the packing density of  $1_n$  in the monolayer can be controlled by the conformational size of the PMAA segment which is variable with the PMAA segment length ( $n$ ) and/or conformational change of the PMAA segment caused by changing the pH.

It is important to estimate an electroactive-site (pinhole) mapping in the resulting monolayers in terms of application to a microelectrode. Quantitative information about the mapping can be extracted by fitting the voltammograms with the theoretical treatment of an array of microelectrodes.<sup>34</sup> Care must be taken in choosing a redox couple for probing the active sites in a monolayer.  $\text{Ru}(\text{NH}_3)_6^{3+/2+}$  has been proposed as a reference redox couple for fast kinetic measurements and has a rate constant and transfer coefficient independent of the electrode metal.

The electrode is assumed to be covered with disk-shaped active sites with an average radius of  $R_a$  and an area fraction of  $1 - \theta$  (where  $\theta$  is the fractional coverage of an inactive (blocking) site). Each active site is surrounded by an inactive area with an average radius of  $R_0$ ; hence, the distance between active sites is  $2R_0$ . For small area fractions of active sites,  $R_a$  and  $R_0$  are related to  $1 - \theta$  by

$$1 - \theta = R_a^2 / R_0^2 \quad (1)$$

Figure 4 shows the results of simulation of a microarray electrode cyclic voltammetry for  $1_{63}$  monolayer-covered electrodes prepared at pHs 3.0 and 8.2. The equations, including eq 1, proposed by Amatore et al.<sup>35</sup> were applied for the simulation of  $i$ - $E$  curves, which is displayed in Figure 4. The overall fit is generally good for both

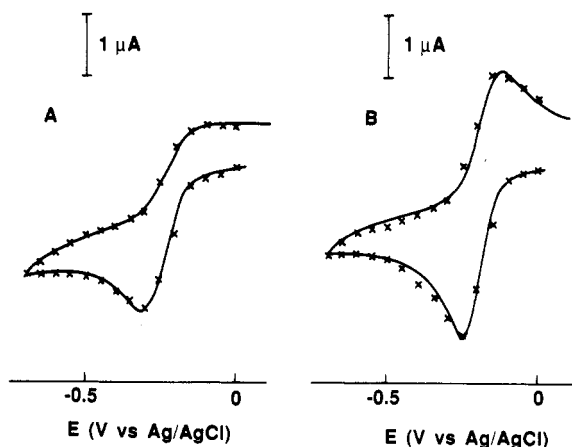


**Figure 4.** Cyclic voltammograms of  $1_{63}$ -coated gold electrodes prepared at pHs 3.0 (A) and 8.2 (B). The solutions are 3 mM  $\text{Ru}(\text{NH}_3)_6^{3+}$  in 1 M KCl, pHs 3.0 and 8.2. The sweep rate is 70 mV/s. Solid curve, experimental cyclic voltammogram; crosses, simulation of microarray electrode cyclic voltammogram (see text).

**Table III**  
Simulated Parameters for Figure 4<sup>a</sup>

	$R_0$ <sup>b</sup> (Å)	$R_a$ <sup>c</sup> (Å)	$1 - \theta$ <sup>d</sup>
prepared at pH 8.2	5000	1120	0.05
prepared at pH 3.0	40	9	0.0005

<sup>a</sup> See Figure 4 for experimental conditions. <sup>b</sup> Average radius of inactive area. <sup>c</sup> Average radius of active area. <sup>d</sup> Area fraction of inactive sites.

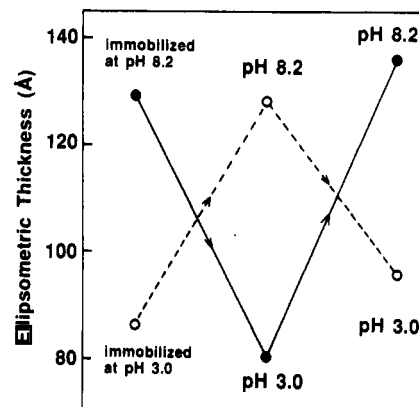


**Figure 5.** Changes in ellipsometric thickness for immobilized monolayers of  $1_{63}$  from pH 3.0 (O) and pH 8.2 (●) solutions by alternately exposing to aqueous solutions of pHs 3.0 and 8.2.

monolayers prepared at pHs 3.0 and 8.2. The parameters  $R_0$ ,  $R_a$ , and  $1 - \theta$  are listed in Table III. There are definite differences in the simulated parameters between adsorption conditions. The monolayer prepared at pH 3.0 gives a smaller active site area ( $R_a$ ) and less area fraction of active site ( $1 - \theta$ ) by a factor of ca.  $10^2$  than that prepared at pH 8.2. This clearly means that the active site area and mapping on the electrode surface are readily and precisely controlled by using the conformational change of the PMAA segment induced with pH.

**pH Responsiveness of the Immobilized Monolayers.** The PMAA segments in the immobilized monolayers on gold substrates are also expected to cause a conformational change with the surrounding pH. Figure 5 shows changes in the ellipsometric thickness of the immobilized monolayers ( $1_{63}$ ) upon alternately exposing to aqueous solutions of pHs 3.0 and 8.2. When the monolayer immobilized at pH 3.0 was treated with pH 8.2 solution, the film thickness increased to a value close to that of the monolayer

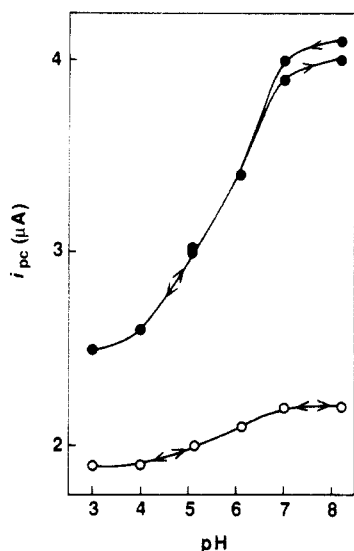


**Figure 6.** pH dependence of  $i_{pc}$  for  $I_{63}$  monolayer-immobilized gold electrodes prepared at pHs 3.0 (○) and 8.2 (●). Experimental conditions are the same as described in Figure 2.

immobilized at pH 8.2 and then reverted almost completely to the original thickness upon treatment with pH 3.0 solution. Reverse trends were observed for the monolayer immobilized at pH 8.2; i.e., the thickness decreased by exposing to pH 3.0 solution and reverted to the original one upon treatment with pH 8.2 solution. These reversible changes in the film thickness would be ascribed to such conformational changes as extension and contraction of the PMAA segments attached to the monolayer surface. Subsequently, the electrochemical response of the  $I_{63}$  monolayer immobilized on a gold electrode induced with pH was examined. Figure 6 displays plots of  $i_{pc}$  for the Fc-Gly redox reaction against pH in the electrolyte solutions. The  $i_{pc}$  values for both monolayers prepared with pHs 3.0 and 8.2 give a marked pH dependence; upon elevating the pH, the  $i_{pc}$  values increase and, in particular, in the pH region 5–7 show a steep increase. This pH region corresponds well with that where PMAA causes the conformational transition from a globular coil to an expanded form. The extent of  $i_{pc}$  change with pH is, however, much less for the monolayer prepared at pH 3.0 relative to that for the monolayer prepared at pH 8.2. As mentioned above, the packing density of  $I_{63}$  on the electrode is affected with pH during the adsorption process, reflecting the conformational size of the PMAA segment. The packing density of  $I_{63}$  in the monolayer adsorbed at pH 3.0 was much higher than that adsorbed at pH 8.2, and thus for the former electrode the blocking ability toward Fc-Gly should be governed mainly by the more tightly packed alkyl chain even though the PMAA segment would cause a conformational change by varying pH in the electrolyte solution. In contrast, for the more loosely packed monolayer such as that adsorbed at pH 8.2, the electrochemical response of Fc-Gly should be affected by the conformational change of the PMAA segment, which consequently led the observed pH dependence of the  $i_{pc}$  value.

## Conclusion

The present study demonstrates that (i) PMAA-functionalized amphiphiles ( $I_n$ ) connected with two long alkyl chains, whose ends are labeled with disulfides, are prepared, (ii)  $I_n$ 's successfully form spontaneously-adsorbed monolayers on gold substrates from aqueous solutions with different pHs, (iii) the adsorption processes as well as the

film thicknesses and lateral molecular orientation of the resulting monolayers are governed by the conformational size and/or the chain length ( $n$ ) of the PMAA segment during adsorption, and (iv) the immobilized monolayer on the gold substrate gives reversible changes in the ellipsometric thickness and in electrochemical response by varying pH, though the latter response is dependent upon the molecular packing density on the electrode. We believe that these findings provide a first example of the preparation of ultrathin polymer films that can control molecularly the thickness and the aggregation state of the component molecules by taking advantage of the conformational change of a polyelectrolyte and that these polymer films are of particular significance not only in view of their applicability for a microarray electrode but also in view of the controlled formation of a two-dimensionally oriented molecular assembly on solid substrates.

## References and Notes

- (1) Olea, A. F.; Thomas, J. K. *Macromolecules* **1989**, *22*, 1165 and references cited therein.
- (2) Pincus, P. *Macromolecules* **1991**, *24*, 2912.
- (3) Borisov, O. V.; Birshtein, T. M.; Zhulina, E. B. *J. Phys. II* **1991**, *1*, 521.
- (4) Ross, R. S.; Pincus, P. *Macromolecules* **1992**, *25*, 2177.
- (5) Zhulina, E. B.; Borisov, O. V.; Birshtein, T. M. *J. Phys. II* **1992**, *2*, 63.
- (6) Niwa, M.; Katsurada, N.; Higashi, N. *Macromolecules* **1988**, *21*, 1878.
- (7) Niwa, M.; Hayashi, T.; Higashi, N. *Langmuir* **1990**, *6*, 263.
- (8) Niwa, M.; Mukai, A.; Higashi, N. *Langmuir* **1990**, *6*, 1432.
- (9) Niwa, M.; Mukai, A.; Higashi, N. *Macromolecules* **1991**, *24*, 3314.
- (10) Higashi, N.; Shiba, H.; Niwa, M. *Macromolecules* **1989**, *22*, 4650.
- (11) Higashi, N.; Shiba, H.; Niwa, M. *Macromolecules* **1990**, *23*, 5297.
- (12) Higashi, N.; Matsumoto, T.; Niwa, M. *J. Chem. Soc., Chem. Commun.* **1991**, 1517.
- (13) Higashi, N.; Nojima, T.; Niwa, M. *Macromolecules* **1991**, *24*, 6549.
- (14) Higashi, N.; Shimoguti, M.; Niwa, M. *Langmuir* **1992**, *8*, 1509.
- (15) Nuzzo, R. G.; Allara, D. L. *J. Am. Chem. Soc.* **1983**, *105*, 4481.
- (16) Li, T. T.-T.; Weaver, M. J. *J. Am. Chem. Soc.* **1984**, *106*, 6107.
- (17) Maoz, R.; Sagiv, J. *Langmuir* **1987**, *3*, 1034.
- (18) Bain, C. D.; Evall, J.; Whitesides, G. M. *J. Am. Chem. Soc.* **1989**, *111*, 7155.
- (19) Widrig, C. D.; Alves, C. A.; Porter, M. D. *J. Am. Chem. Soc.* **1991**, *113*, 2805.
- (20) Collard, D. M.; Fox, M. A. *Langmuir* **1991**, *7*, 1192.
- (21) Higashi, N.; Mori, T.; Niwa, M. *J. Chem. Soc., Chem. Commun.* **1990**, 225.
- (22) Niwa, M.; Mori, T.; Higashi, N. *J. Mater. Chem.* **1992**, *2*, 245.
- (23) Niwa, M.; Shimoguchi, M.; Higashi, N. *J. Colloid Interface Sci.* **1992**, *145*, 592.
- (24) Finkea, H. O.; Robinson, L. R.; Blackburn, A.; Richter, B.; Allara, D.; Bright, T. *Langmuir* **1986**, *2*, 239.
- (25) Finkea, H. O.; Avery, S.; Lynch, M.; Furtch, T. *Langmuir* **1987**, *3*, 409.
- (26) Sabatini, E.; Rubinstein, I.; Maoz, R.; Sagiv, J. *J. Electroanal. Chem.* **1987**, *219*, 365.
- (27) Sabatini, E.; Rubinstein, I. *J. Phys. Chem.* **1987**, *91*, 6663.
- (28) Rubinstein, I.; Steinberg, S.; Tor, Y.; Shanzer, A.; Sagiv, J. *Nature* **1988**, *332*, 426.
- (29) Porter, M. D.; Bright, T. B.; Allara, D. L.; Chidsey, C. E. D. *J. Am. Chem. Soc.* **1987**, *109*, 3559.
- (30) Niwa, M.; Higashi, N.; Shimizu, M.; Matsumoto, T. *Makromol. Chem.* **1988**, *189*, 2187.
- (31) Renoll, M.; Newman, M. S. *Org. Synth.* **1971**, *Collect. Vol. 3*, 503.
- (32) Oth, A.; Doty, P. *J. Phys. Chem.* **1952**, *56*, 43.
- (33) Bard, A. J.; Faulkner, L. R. *Electrochemical Methods: Fundamentals and Applications*; Wiley: New York, 1980.
- (34) Finkea, H. O.; Snider, D. A.; Fedyk, J. *Langmuir* **1990**, *6*, 371.
- (35) Amatore, C.; Savéant, J. M.; Tessier, D. *J. Electroanal. Chem.* **1983**, *147*, 39.